CHAPTER 4

CROTON PERSIMILIS EXTRACT: NATURAL CORROSION INHIBITOR FOR MILD STEEL IN ACID MEDIA

This chapter presents preliminary phytochemical screening, metal-binding ability and corrosion inhibition properties of ethanolic leaf extract of *Croton persimilis* (CPE). *Croton persimilis* belongs to Euphorbiaceae family. The anti-corrosion effect of CPE in 1 M HCl and 0.5 M H_2SO_4 for mild steel has been explored by physicochemical, electrochemical and surface morphological studies. The major constituents present in the extract are neocrotocembraneic acid and stigmasterol[158]. There are various other minor constituents comprised, possessing either synergistic or antagonistic effects. Nevertheless, in this work, only significant components are regarded as the compounds accountable for corrosion inhibition. Major components of *Croton persimilis* leaves, neocrotocembraneic acid and stigmasterol have been subjected to quantum mechanical studies to evaluate the plant leaves' anti-corrosion effect. Structures of neocrotocembraneic acid and stigmasterol are shown in Fig. 4.1.

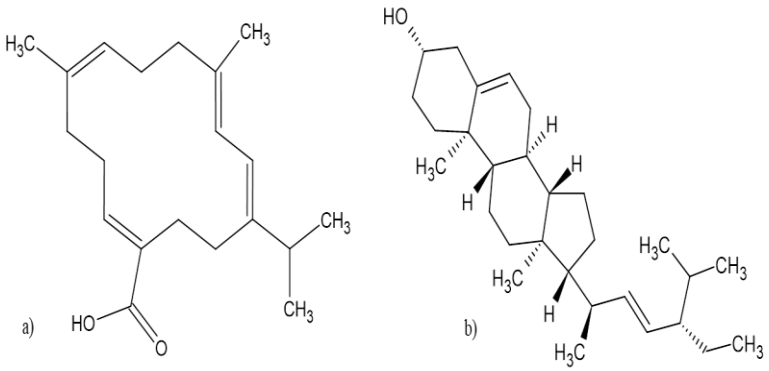

Fig. 4.1: Structures of a) neocrotocembraneic acid
b) stigmasterol

Croton persimilis

Results and Discussions

Phytochemical screening of CPE

The presence of various phytochemicals in CPE confirmed using different tests, and the results are summarised in Table 4.1

Table 4.1: Phytochemical screening of CPE

Sl. No.	Compounds	Tests	Results
1	Alkaloids	Mayers reagent	−−
2	Steroids	Salkowaski's test	++
3	Phenolic compounds	Potassium ferrocyanide test	++
4	Flavanoids	Sodium hydroxide test	++
5	Saponins	Froth test	++
6	Tannins	Lead acetate test	−−
7	Cardiac glycosides	Conc. sulphuric acid test	++
8	Coumarin	Alcoholic NaOH test	++
9	Quinones	Conc. sulphuric acid test	++

++ (present), − − (Absent)

FTIR spectroscopy

Predominant functional groups present in CPE were recognized by recording FTIR spectroscopy of CPE, shown in Fig. 4.2.

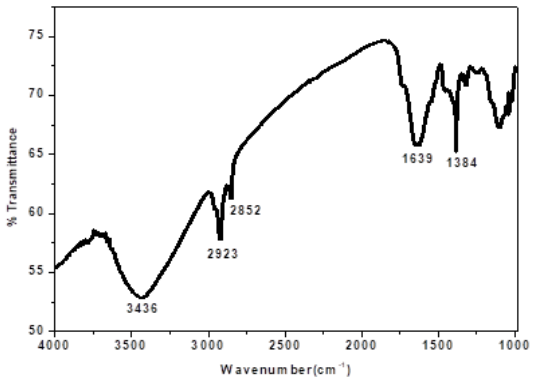

Fig. 4.2: FTIR spectrum of CPE

Broadband at 3436 cm^{-1} represents O-H stretching vibration. The two sharp peaks at 2923 cm^{-1} and 2852 cm^{-1} correspond to alkyl C-H stretching bonds. Alkyl and aromatic C=C stretching vibrations are indicated by the bands at 1639 cm^{-1} and

1384 cm^{-1}, respectively. The other prominent peaks reveal the existence of other constituents present in the CPE.

Weight loss measurements

❖ ***Effect of concentration***

Weight loss measurements reckon corrosion inhibition efficiency (η%) and corrosion rate (υ) on mild steel in acidic media such as 1 M HCl and 0.5 M H_2SO_4 with and without various concentrations (1-5 v/v %) of CPE have been recorded in Table 4.2. It was evident that an increment in inhibition capacity occurs in increasing the inhibitor concentration for both the acid solutions. It was observed that CPE is an excellent corrosion inhibitor in 0.5 M H_2SO_4, having maximum inhibition efficiency at 5 v/v% as 98.09%. In HCl medium, it was attained an extreme efficiency of 86.45% at 5 v/v%. The higher inhibition power in H_2SO_4 than HCl may attribute to the sufficient availability of metal sites on the surface of mild steel. It is because of the lesser adsorption of sulfate ions on the metal surface. Hence, the number of adsorbed organic molecules of inhibitor CPE on mild steel is more in the H_2SO_4 medium.

Table 4.2: Weight loss measurements of mild steel with and without CPE in 1 M HCl and 0.5 M H_2SO_4 at room temperature for 24 hrs

Conc. (v/v %)	Corrosion rate (mm/yr)		Inhibition efficiency (η%)	
	1 M HCl	0.5 M H_2SO_4	1 M HCl	0.5 M H_2SO_4
Blank	3.95	35.57	-	-
1	1.21	3.03	69.3	91.45
2	0.88	1.45	77.6	95.90
3	0.66	1.03	83.2	97.08
4	0.55	0.91	85.8	97.42
5	0.53	0.67	86.4	98.09

❖ ***Effect of temperature***

Temperature studies on the corrosion process have a crucial role in analyzing the stability of adsorbed film of inhibitor molecules on the mild steel surface. The extent of

decay is dependent on temperature and becomes severe in acidic media. In the present investigation, the influence of temperature on the corrosion inhibition was carried out by weight loss measurements for 24 hrs in 1 M HCl and 0.5 M H_2SO_4 by adding different concentrations of CPE at a temperature range of 303-333 K. The variation of corrosion inhibition efficiency with temperature is tabulated in Table 4.3. It is graphically represented in Fig. 4.3.

Table 4.3: Corrosion rate (υ) and inhibition efficiency (η%) of CPE in 1 M HCl and 0.5 M H_2SO_4 at different temperatures for 24 hrs

Medium	Conc. (v/v %)	υ (303 K)	η% (303 K)	υ (313 K)	η% (313 K)	υ (323 K)	η% (323 K)	υ (333 K)	η% (323 K)
1 M HCl	Blank	3.95	-	13.11	-	22.05	-	31.77	-
	1	1.21	69.36	8.07	38.44	14.06	36.23	23.41	26.31
	2	0.88	77.72	3.38	74.21	8.32	62.26	16.36	48.50
	3	0.66	83.29	2.19	83.29	5.94	73.06	12.56	60.46
	4	0.55	86.07	1.88	85.65	4.66	78.86	11.92	62.48
	5	0.53	86.58	1.76	86.57	4.49	79.63	11.69	63.20
0.5 M H_2SO_4	Blank	35.57	-	58.27	-	86.25	-	106.2	-
	1	3.03	91.48	15.7	73.05	33.39	61.28	48.95	53.93
	2	1.45	95.92	11.05	81.03	27.54	68.06	38.47	63.79
	3	1.03	97.10	6.27	89.23	18.94	78.04	28.65	73.03
	4	0.91	97.44	2.05	96.48	12.36	85.66	22.59	78.74
	5	0.67	98.11	0.74	98.73	7.92	90.81	16.52	84.45

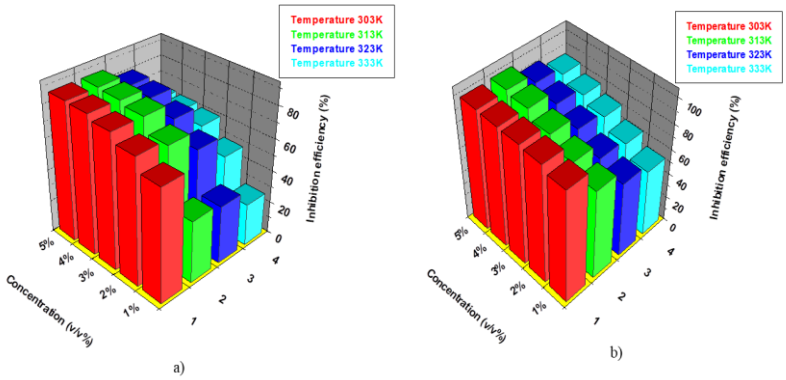

Fig. 4.3: Variation in inhibition efficiency of CPE in a) 1 M HCl b) 0.5 M H_2SO_4 at elevated temperatures

Fig. 4.3 expressed that the corrosion inhibition power of CPE decreased with an increase in temperature for the same concentration. This trend is because of the

destruction of the adsorbed film on the metal surface when the temperature rises. Protecting power of CPE in 0.5 M H_2SO_4 was 84.45% at extreme concentration and temperature understudy, whereas in 1 M HCl, it was decreased to 63.20% at the same concentration and temperature.

log K vs 1/T plots for mild steel coupons in acid solutions with and without CPE can be drawn with the help of Arrhenius equation (41), and they are shown in Fig. 4.4 a) and Fig. 4.5 a). From the curves' slope, the activation energy for the metal corrosion in 1 M HCl and 0.5 M H_2SO_4 was derived. Thermodynamic parameters such as enthalpy of activation (ΔH^*) and entropy of activation (ΔS^*) were calculated using transition state theory. Plots of log K/T vs 1/T for metal corrosion in 1 M HCl and 0.5 M H_2SO_4 are shown in Fig. 4.4 b) and Fig. 4.5 b). The calculated values of properties such as activation energy (E_a), enthalpy of activation (ΔH^*) and entropy of activation (ΔS^*) are given in Table 4.4. On comparing the activation energy of corrosion with and without CPE, it was clear from the table that its value is higher in the presence of CPE. In contrast, it is lower in the absence of CPE for both acid solutions. The positive value of enthalpy revealed the endothermic behaviour of metal corrosion reactions. On close examination of E_a and ΔH^* values at a maximum concentration of 5 v/v%, it was clear that metal corrosion has experienced higher activation energy and enthalpy of activation in 0.5 M H_2SO_4 medium. This data dramatically justifies CPE molecules being more strongly adsorbed on the mild steel surface in 0.5 M H_2SO_4 than 1 M HCl. As the concentration of CPE increases, the values of ΔS^* also increases. Entropy of activation for corrosion was seen to be positive in the presence of CPE, which indicated that the activated complex's randomness is more than the reactants in both acid solutions. But the increase in randomness was more facilitated in H_2SO_4 than HCl medium.

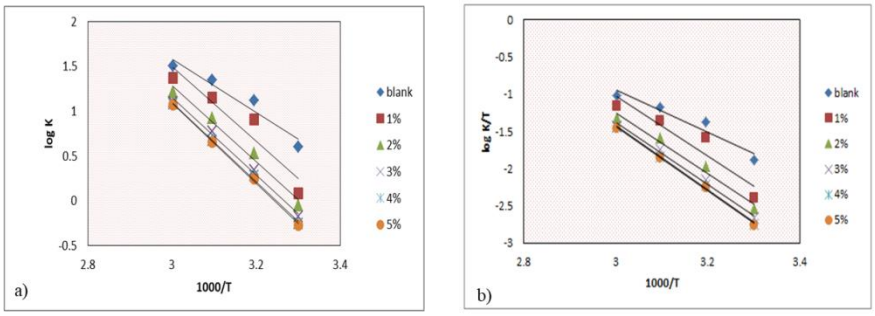

Fig. 4.4: Arrhenius plots of a) log K vs 1000/T b) log K/T vs 1000/T with and without CPE in 1 M HCl

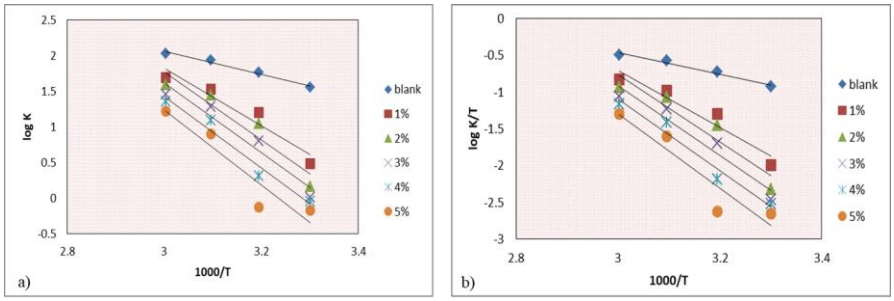

Fig. 4.5: Arrhenius plots of a) log K vs 1000/T b) log K/T vs 1000/T with and without CPE in 0.5 M H_2SO_4

Table 4.4: Thermodynamic parameters of mild steel corrosion with and without CPE in 1 M HCl and 0.5 M H_2SO_4

Medium	Conc. (v/v %)	E_a (kJ mol^{-1})	A	ΔH^* (kJ mol^{-1})	ΔS^* (J $mol^{-1}K^{-1}$)
1 M HCl	Blank	57.24	3.58×10^{10}	54.6	-44.7842
	1	79.91	1.04×10^{14}	77.3	17.68331
	2	81.42	1.10×10^{14}	78.8	22.01056
	3	82.71	1.29×10^{14}	80.1	23.29342
	4	85.14	2.76×10^{14}	82.5	27.56323
	5	85.80	3.40×10^{14}	83.2	27.67812
0.5 M H_2SO_4	Blank	30.96	8.17×10^{6}	28.3	-114.51
	1	76.98	7.62×10^{13}	74.3	18.94702
	2	91.02	1.06×10^{16}	88.4	59.97935
	3	93.66	1.94×10^{16}	91.0	65.01504
	4	95.95	2.88×10^{16}	93.3	68.28921
	5	100.14	8.34×10^{16}	97.5	77.13518

Adsorption isotherms

Adsorption isotherms provide authentic facts concerning the interaction between inhibitor molecules and mild steel. The mechanism of corrosion inhibition is blocking the rate of cathodic reaction or hindering the anodic metal dissolution or both by the adsorption of inhibitor molecules on the surface of the metal. Among various isotherms

such as Langmuir, El-Awady, Frumkin, Temkin, Freundlich and Flory-Huggins isotherms, the most suitable isotherm in both acid media was Langmuir isotherm, which was found by correlation coefficient (R^2). Langmuir adsorption isotherms of CPE on mild steel surface in 1 M HCl and 0.5 M H_2SO_4 at room temperature are shown in Fig. 4.6. R^2 values were seen to be very close to unity in both acids.

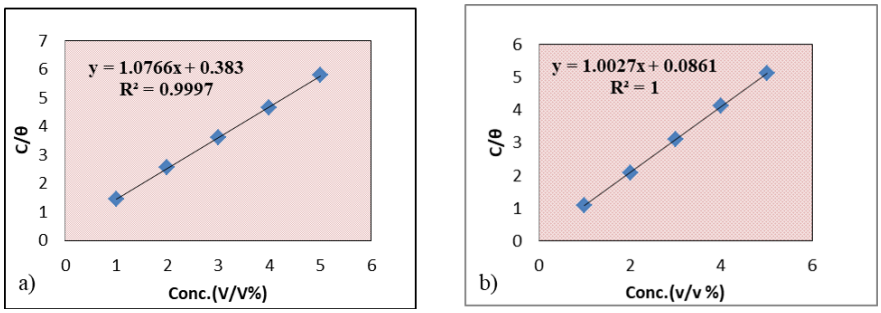

Fig. 4.6: Langmuir adsorption isotherm of CPE on mild steel in a) 1 M HCl b**)** 0.5 M H_2SO_4 at room temperature

ΔG^0_{ads} value determines the interaction between the charged molecule and the charged metal surface. In the present study, CPE on mild steel in 1 M HCl and 0.5 M H_2SO_4 exhibited ΔG^0_{ads} -29.73 and -33.47 $kJmol^{-1}$, respectively, indicating that CPE adsorbed on the metal surface by both electrostatic and chemical interaction[92].

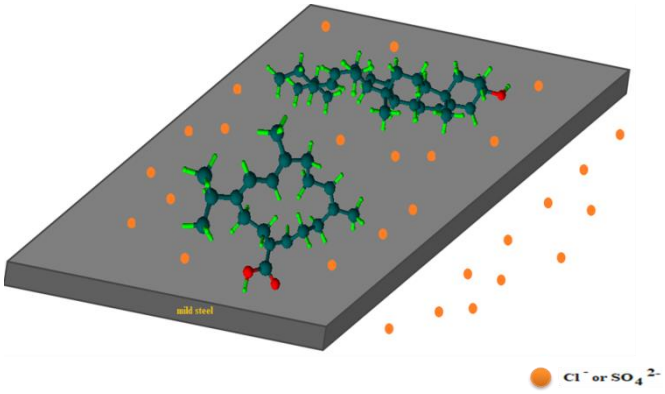

Fig. 4.7: Interaction diagram between CPE molecules and mild steel surface in acid media

Expected mechanism of corrosion inhibition of CPE on mild steel surface in acid is depicted in Fig. 4.7. Major components of CPE are neocrotocembraneic acid, stigmasterol. It may be suggested that the chief constituents of CPE adsorb on the metal

surface mainly by transferring electrons from oxygen atoms in –COOH and –OH functional groups and by the interaction with the unsaturated bonds.

UV-Visible spectroscopy

UV-Visible spectra were plotted to ascertain the metal-binding ability of CPE using various metal salt solutions shown in Fig. 4.8. UV spectrum of CPE exhibited a maximum absorbance of 0.279 at 404 nm and also an absorbance of 0.116 at 664 nm. There was a sharp decrease in CPE intensity after binding with all the metal salts used for the study. In $CoCl_2$, maximum absorbance of 0.165 at 402 nm showed 40% decrease in the intensity after binding. Chromium (III) acetate displayed maximum absorbance of 0.176 at 403 nm, which means 37% decrease in the intensity. For Mn(II) acetate maximum absorbance observed was 0.178 at 402 nm, which disclosed 36% decrease in the intensity after binding. NaCl and Zn(II) acetate showed a significant decrease in intensity as the maximum absorbance observed was 0.076 at 400 nm and 0.041 at 403 nm, respectively. Cu(II) acetate and Fe(III) chloride exhibit maximum absorbance of 0.039 at 662 nm and 0.026 at 661 nm, respectively. The decrease in intensity due to quenching may attribute to its strong affinity towards metal salts[146].

Electrochemical impedance spectroscopy

Analysis of impedance behaviour was conducted by an alternate current method such as electrochemical impedance spectroscopy, which helped evaluate current-potential responses at the metal/solution interface. Randle's circuit (Fig. 1.8) was acted as an equivalent circuit in the present work, including solution resistance R_s, charge transfer resistance R_{ct} and double layer capacitance C_{dl}. Regular and routine metal surface implies the ideal dielectric property of the metal. If there is any misshape in the metal surface, it will deviate from its ideal dielectric behaviour. So, a constant phase element is compensated for C_{dl}.

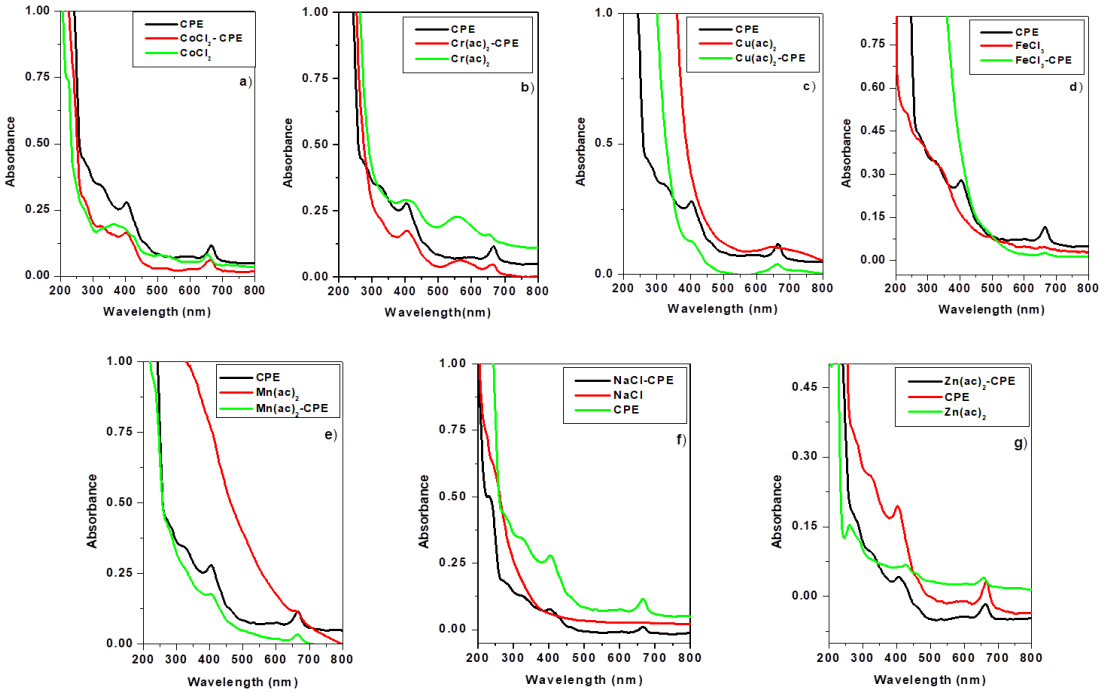

Fig. 4.8: UV spectra of a) CPE, $CoCl_2$ and CPE.$CoCl_2$ b**)** CPE, $Cr(ac)_2$ and CPE.$Cr(ac)_2$ c**)** CPE, $Cu(ac)_2$ and CPE.$Cu(ac)_2$ d**)** CPE, $FeCl_3$ and CPE.$FeCl_3$ e**)** CPE, $Mn(ac)_2$ and CPE.$Mn(ac)_2$ f**)** CPE, NaCl and CPE.NaCl g**)** CPE, $Zn(ac)_2$ and CPE.$Zn(ac)_2$

Impedance spectra include Nyquist and Bode plots for mild steel in 1 M HCl and 0.5 M H_2SO_4 by adding varying concentrations (0-5 v/v %) of the inhibitor CPE at room temperature are shown in Fig. 4.9 & 4.10. Impedance parameters gained from the impedance spectra for both media are given in Table 4.5. The highest semicircle was attained with a concentration of 5 v/v %; it successively decreased as the concentration decreases. This decreasing trend implied that as CPE concentration increases, the impedance of inhibited mild steel raised and lowered its corrosion rate.

From Table 5, it has been evident that charge transfer resistance (R_{ct}) was increased with CPE concentration. In contrast, double-layer capacitance (C_{dl}) was lowered, which indicated that the thickness of the electrical double layer increases with the concentration[74]. The increase in R_{ct} values predominant in the H_2SO_4 medium

pointed out that CPE molecules strongly resisted the charge transfer reaction of corrosion in that medium, which can be considered the rate-determining reaction.

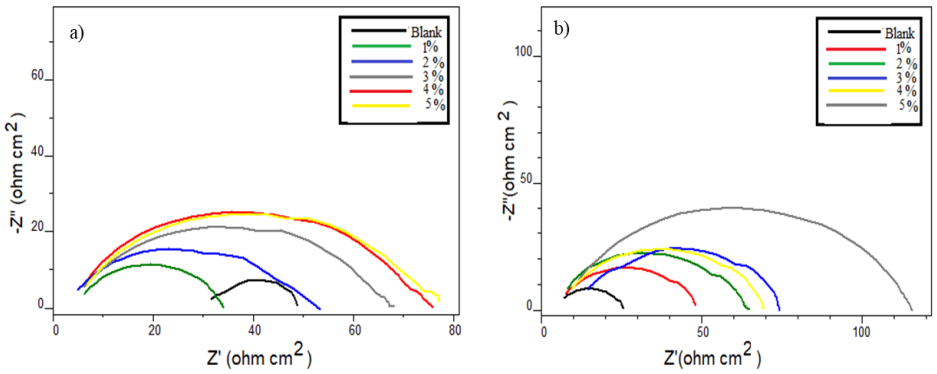

Fig. 4.9: Nyquist plots of mild steel with ad without CPE in a) 1 M HCl and b) 0.5 M H_2SO_4

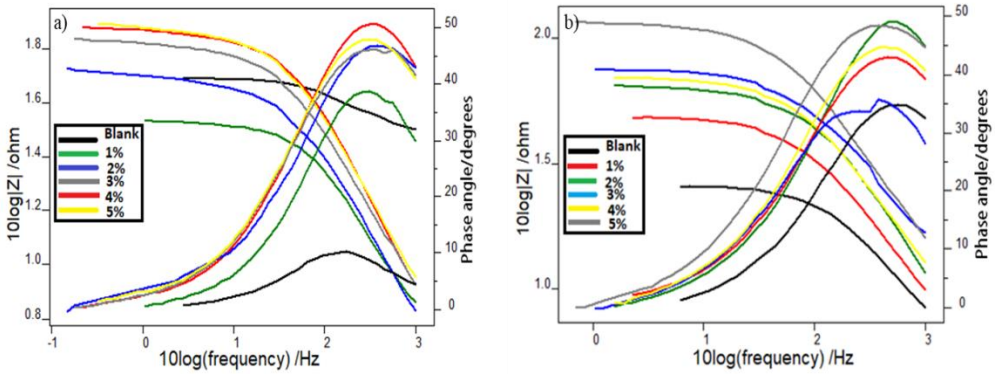

Fig. 4.10: Bode plots of mild steel with and without CPE in a) 1 M HCl and b) 0.5 M H_2SO_4

Table 4.5: Impedance parameters of mild steel in 1 M HCl and 0.5 M H_2SO_4 with and without CPE

Conc. (v/v %)	1 M HCl			0.5 M H_2SO_4		
	R_{ct} (Ωcm^2)	C_{dl} (μ Fcm^{-2})	η_{EIS}%	R_{ct} (Ωcm^2)	C_{dl} (μ Fcm^{-2})	η_{EIS}%
Blank	15.7	78.75	-	18.1	47.39	-
1	25.6	67.70	38.67	37.4	40.87	51.60
2	38.5	69.31	59.22	51.3	27.21	64.71
3	53.1	64.13	70.43	54.2	32.29	66.60
4	60.2	49.23	73.92	54.7	31.00	66.91
5	60.7	55.30	74.13	92.9	26.18	80.51

Decreasing trend of C_{dl} values is on account of the adsorption of inhibitor molecules on the mild steel surface. The decrease in C_{dl} value was more in the case of 0.5 M H_2SO_4, which showed an increase in surface coverage by CPE. It caused higher

inhibition potency in H_2SO_4 than in the HCl medium. Maximum inhibition efficiency of 74.13% and 80.51% was found at 5% concentration of CPE in 1 M HCl and 0.5 M H_2SO_4, respectively. This result was also in line with the data from weight loss measurements.

Potentiodynamic polarization studies

The potentiodynamic polarization curves such as Tafel plots (Fig. 4.11) and linear polarization plots (Fig. 4.12) of mild steel in 1 M HCl and 0.5 M H_2SO_4 with and without CPE are used to determine the polarization data, such as the corrosion current density (i_{corr}), the potential of corrosion (E_{corr}) current, cathodic slope (b_c), anodic slope (b_a), and inhibition power (η_{pol}%) which are given in Table 4.6. The polarization data showed that with the addition of inhibitor CPE, corrosion current density gets reduced. It can be ascribed to the interference in the anodic or cathodic process of corrosion or both. Thus, corrosion inhibition potency increased significantly in both acids. The inhibition efficiency of CPE for mild steel attained 80.88% in 1 M HCl and 84.09% in 0.5 M H_2SO_4 at the highest concentration under study. From Tafel plots in Fig.4.11, it is clear that both cathodic and anodic slopes were disturbed in a uniform manner which indicated the mixed type inhibition character of CPE in 1 M HCl and 0.5 M H_2SO_4, i.e., CPE behaves as an anodic and cathodic inhibitor[71].

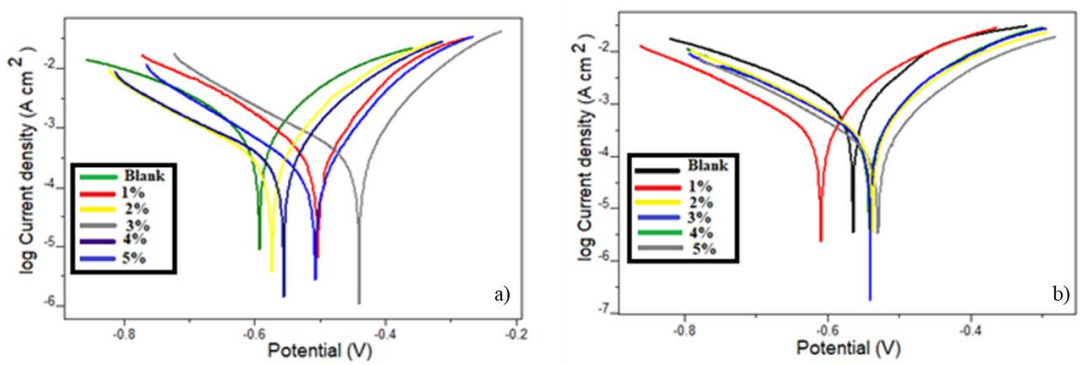

Fig. 4.11: Tafel plots of mild steel with and without CPE in a) 1 M HCl and b) 0.5 M H_2SO_4

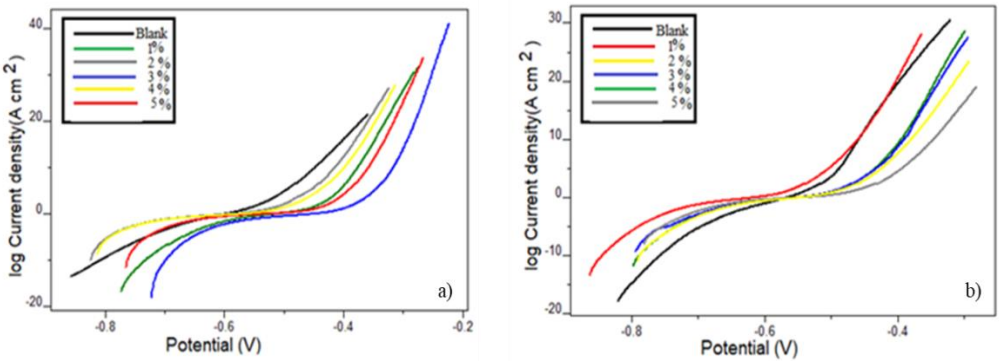

Fig. 4.12: Linear polarization plots of mild steel with and without CPE in a) 1 M HCl and b) 0.5 M H_2SO_4

Table 4.6: Potentiodynamic polarization parameters of mild steel in 1 M HCl and 0.5 M H_2SO_4 with and without CPE

Medium	Conc. (v/v%)	Tafel data					Polarization data	
		$-E_{corr}$ (mV)	i_{corr} ($\mu A/cm^2$)	b_a (mV/dec)	$-b_c$ (mV/dec)	$\%\eta_{pol}$	R_p (ohm)	$\%\eta_{Rp}$
1 M HCl	Blank	597.9	1240	166	221	-	33.14	-
	1	513.6	549.9	111	164	55.64	51.68	35.87
	2	607.7	398.8	138	173	67.82	72.97	54.58
	3	466.8	390.4	107	169	68.54	83.61	60.36
	4	589.2	364.9	132	185	70.56	91.77	63.88
	5	529.3	236.7	106	151	80.88	113.9	70.90
0.5 M H_2SO_4	Blank	602.2	1616	184	193	-	25.30	-
	1	645.1	576.6	153	150	64.29	56.95	55.57
	2	571.7	491.2	147	156	69.61	76.80	67.05
	3	575.4	486.3	141	160	69.92	86.96	70.90
	4	574.5	459.1	135	151	71.59	97.47	74.04
	5	560.9	256.9	131	143	84.09	115.7	78.13

Electrochemical noise measurements

Fig. 4.13 delineates the current noise for mild steel in the absence and presence of three different CPE concentrations (1, 3, 5 v/v %) in 1 M HCl and 0.5 M H_2SO_4. It is evident that when the concentration of CPE increased, its protecting power was also raised. The current and potential noise for the inhibited system was lower than the uninhibited system. The potential noise signal for the higher concentration of CPE (5 v/v%) was positioned at a lower magnitude, showing corrosion inhibition by the inhibitor. The signal was at a higher magnitude for uninhibited acid media, indicating appreciable localized metallic corrosion on the metal surface[154].

Power spectral density (PSD) plots originated from the frequency domain analysis of noise, shown in Fig. 4.14. Comparing the magnitude of the current noise signals for blank metal with inhibited metal was lower for the metal dipped in acid solution with various concentrations of CPE (1, 3, 5 v/v %) than the uninhibited acid solution. It connoted an appreciable amount of localized corrosion on the mild steel surface immersed in the uninhibited acid solution. For the highest concentration (5 v/v%), the magnitude of the current noise signals was attained the most negligible value suggesting its good corrosion inhibition nature and its value increasing as concentration decreased.

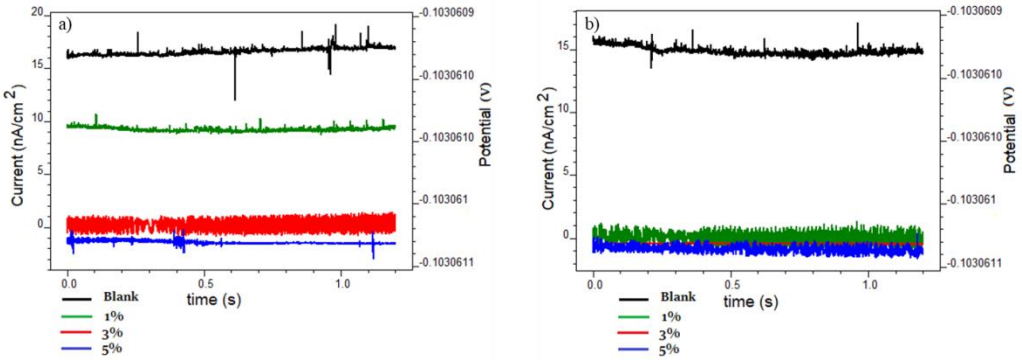

Fig. 4.13: Current noise plots of mild steel with and without CPE in a) 1 M HCl b) 0.5 M H_2SO_4

Pitting corrosion resistance power can be expressed by examining pitting index curves (Fig. 4.15). Contrary to PSD plots, the amplitude of the pitting index curve for blank metal was lower than the metal in the inhibited acid solution. It may be attributed to the worst mitigation to pitting corrosion offered by blank metal treated in an uninhibited acid medium. Pitting index value of the mild steel immersed in 1 M HCl containing 5 v/v% CPE solution was recorded smaller than that in 0.5 M H_2SO_4 solution having the same concentration of CPE. At the same time, pitting index value of the mild steel in the blank solutions of 1 M HCl and 0.5 M H_2SO_4 were observed to be smaller than inhibited metal.

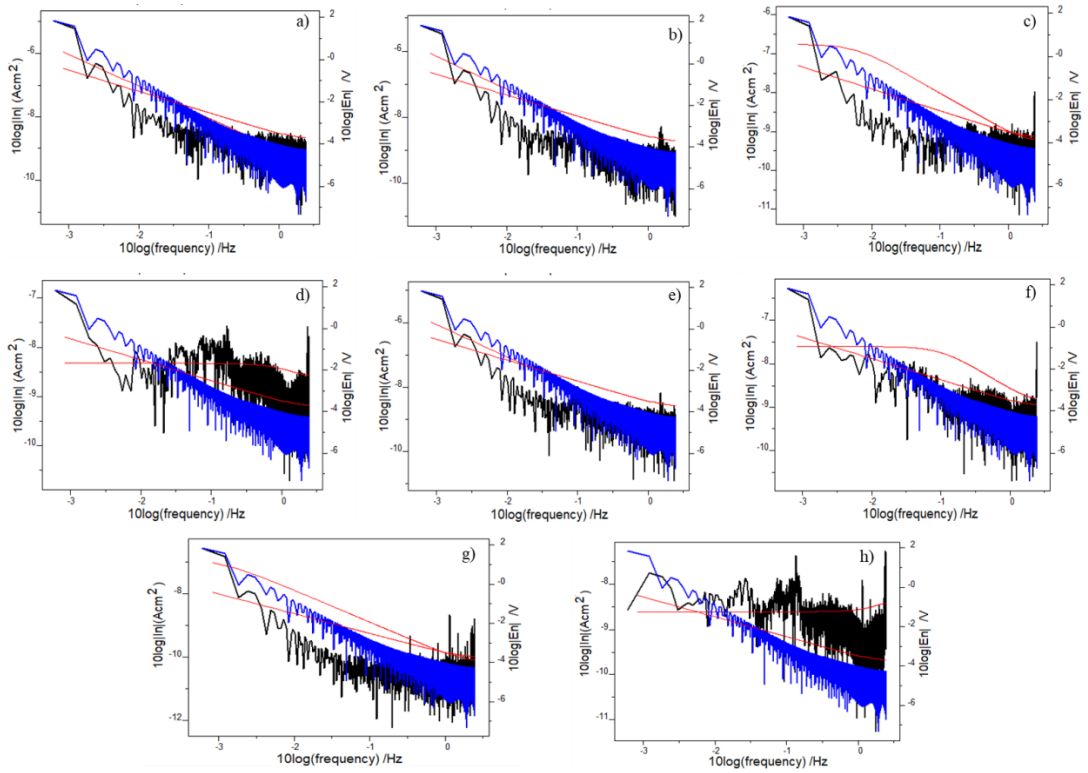

Fig. 4.14: Power spectral density plots of mild steel in 1 M HCl a) without CPE b) 1% CPE c) 3% CPE d) 5% CPE; Power spectral density plots of mild steel in 0.5 M H_2SO_4 e) without CPE f) 1% CPE g) 3% CPE h) 5% CPE

Scanning electron microscopy

Surface morphological studies can reinforce the adsorption mechanism by the inhibitor molecules of CPE on mild steel surfaces. Fig. 4.16 a) exhibits the SEM image of the surface of shining mild steel. Fig. 4.16 b), c), d) and e) reveals the SEM images of the surface of mild steel metal after the period of immersion in 1 M HCl and 0.5 M H_2SO_4, respectively, in the absence and presence of CPE. From Fig. 4.16, it was evident that the surface of the mild steel metal is seriously affected by the rust in the absence of the inhibitor CPE. It could be examined that the surface corrosion is lower in H_2SO_4 solution in the presence of CPE, and the surface is more transparent and refined in it than in the HCl solution. So it can be realized that CPE acts as an efficient green corrosion inhibitor in acidic media[159].

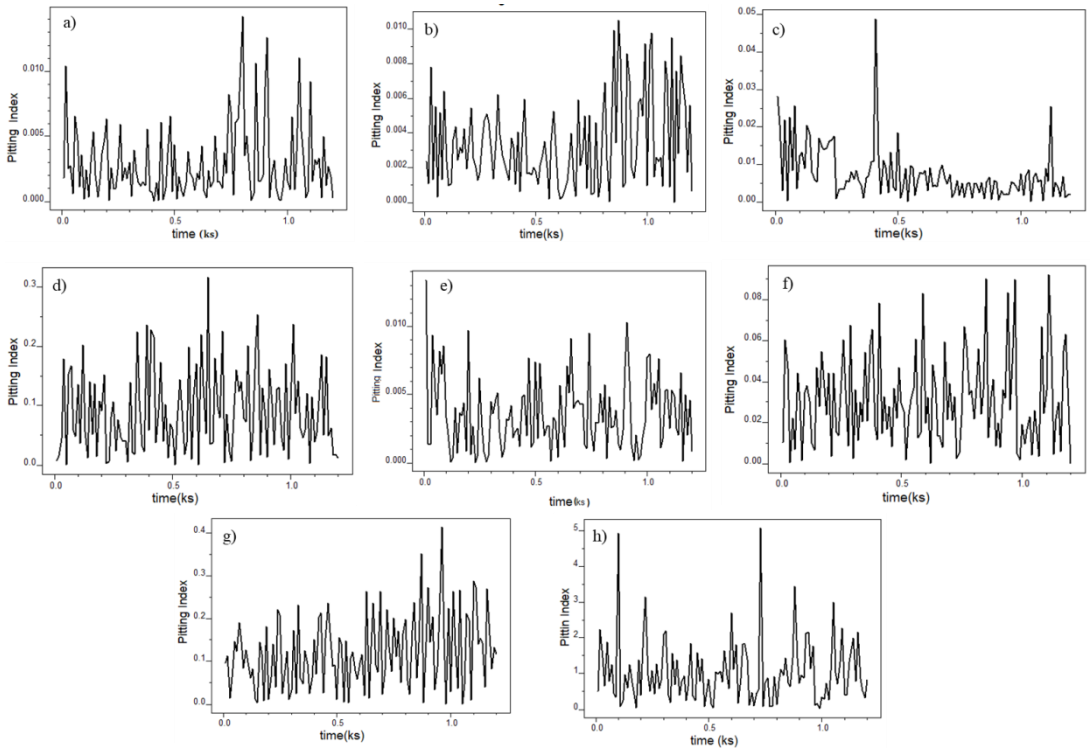

Fig. 4.15: Pitting index curves of mild steel in 1 M HCl a) without CPE b) 1% CPE c) 3% CPE d) 5% CPE; Pitting index curves of mild steel in 0.5 M H_2SO_4 e) without CPE f) 1% CPE g) 3% CPE h) 5% CPE

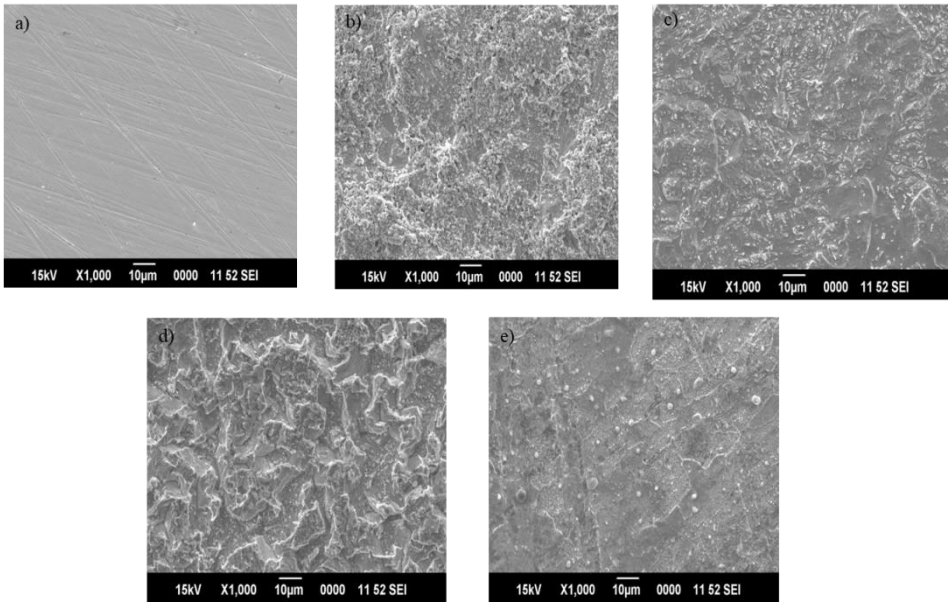

Fig. 4.16: SEM images of the surface of mild steel a) bare b) in 1 M HCl c) in 1 M HCl with CPE d) in 0.5 M H_2SO_4 e) in 0.5 M H_2SO_4 with CPE

Quantum mechanical calculations

Quantum mechanical parameters like E_{HOMO}, E_{LUMO}, ΔE, Ionisation energy (I), Electron affinity (A), chemical potential (μ), electronegativity (χ), hardness (η) and the

number of transferred electrons (ΔN) of neocrotocembraneic acid and stigmasterol are computed in Table 4.7. The optimized geometry, HOMO and LUMO pictures of neocrotocembraneic acid and stigmasterol are portraited in Fig. 4.17.

Table 4.7: Quantum mechanical parameters (in eV) of neocrotocembraneic acid (I) and stigmasterol (II)

Molecule	E_{HOMO}	E_{LUMO}	ΔE	I	A	μ	χ	η	ΔN
I	-2.135	1.081	3.21	2.13	-1.081	-0.527	0.52	1.608	2.01
II	-3.129	1.125	4.25	3.12	-1.125	-1.002	1.00	2.127	1.40

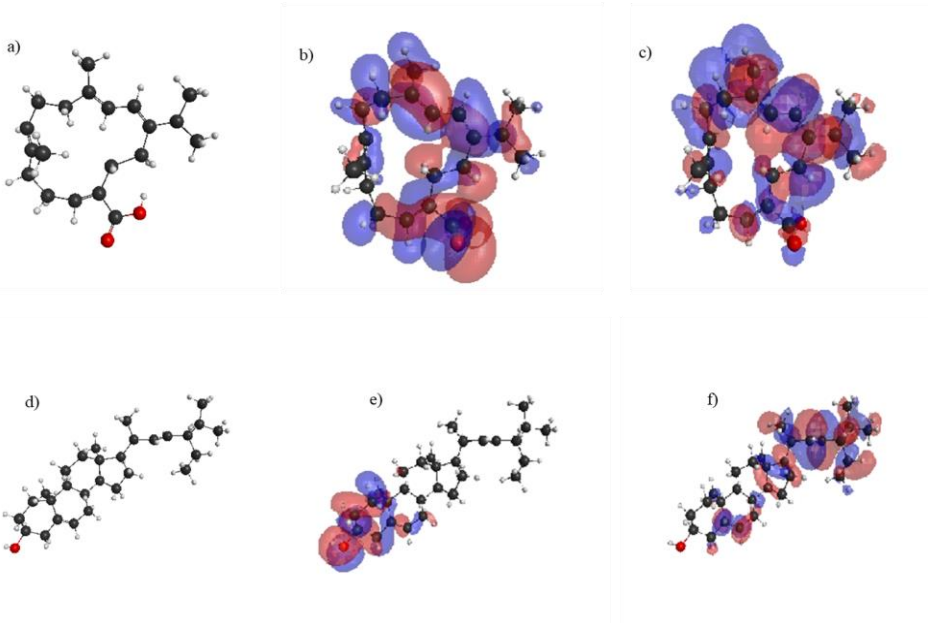

Fig. 4.17: a) Optimized geometry, b) HOMO and c) LUMO of neocrotocembraneic acid; d) Optimized geometry, e) HOMO and f) LUMO of stigmasterol

Adsorption of an inhibitor molecule on the metal surface is quantified by the value of change in energy (E_{LUMO} - E_{HOMO}). The ΔE value was low for neocrotocembraneic acid, facilitating the low energy condition for the transfer of electrons from HOMO of neocrotocembraneic acid to the vacant orbitals of Fe. This low ΔE value of 3.216 eV of neocrotocembraneic acid implies that CPE has significant protection efficiency. The ΔN values impart the concept concerning the relation between donor-acceptor molecules. If the value of ΔN is less than 3.6, the inhibitor molecules

tend to donate electrons to the metal surface[160]. Here the fraction of electrons transferred in neocrotocembraneic acid was 2.012, and for stigmasterol, it is 1.409. Presence of a conjugated double bond in neocrotocembraneic acid may enhance the donation of electrons to the metal surface. It may attribute to the high inhibition capacity of the major components. Thus, in turn, substantiates agreement between theoretical and experimental results.

Statistical analysis

❖ ***Optimization of factors for inhibition efficiency (IE%)***

Response surface methodology (RSM) yields optimized conditions concerning input values to acquire a proper response. From weight loss measurements, it was clear that the corrosion inhibition efficiency of CPE depends on its concentration and working temperature, and effective inhibition was obtained in 0.5 M H_2SO_4 than 1 M HCl medium. So, corrosion inhibition efficiency of the inhibitor and variables such as temperature and concentration of CPE in 0.5 M H_2SO_4 medium were connected through regression analysis. Parameters of the RSM technique are temperature in K (X_1) and concentration of CPE in v/v% (X_2).

The influence of temperature (X_1) and concentration of CPE (X_2) on inhibition efficiency (IE%) was described by a central composite design (CCD). There were nine experimental runs in CCD to optimize the parameters, which are given in Table 4.8. A full quadratic model was assigned to represent the inhibitor efficiency in response to the independent parameters in selected ranges:

$$IE = 2490 - 14.10X_1 - 7.81X_2 + 0.02027X_1^2 - 0.765X_2^2 + 0.0605X_1X_2 \quad (52)$$

Validity of this quadratic model can be verified using Residual plots shown in Fig. 4.18. On close observation of the normal probability plot, it has been seen that the response model for inhibition efficiency was fixed to the normal distribution. It suggests

that the established model required no response transformation, and there are no detectable problems with normality. Versus fits plot conveyed that there is a constancy in the variance of observations for all responses. Histogram of residuals indicated that the residuals are distributed uniformly for all frequencies[161]. Points of observed runs were distributed randomly within the fixed residuals, which authenticated the model's precision, and was established by Versus order plot. In short, all the plots in this figure verified the validity of the model to explain the inhibition efficiency of the inhibitor CPE.

Table 4.8: Experimental and predicted IE% from the weight loss measurements and CCD

Temp (X_1)	Conc. (X_2)	IE%		Residual
		Experimental	Predicted	
313	5	98.73	99.03913	0.30913
333	1	53.93	53.99153	0.06153
313	1	73.05	72.89313	-0.15687
333	5	84.45	84.97753	0.52753
313	3	89.23	89.02613	-0.20387
323	5	90.81	89.98133	-0.82867
333	3	73.03	72.54453	-0.48547
323	1	61.28	61.41533	0.13533
323	3	78.04	78.75833	0.71833

Table 4.9 explains the analysis of variance for corrosion inhibition efficiency. P-value determines whether the effect for that variable is significant or not. The selected value of α, degree of essentialness, was 0.05. Table 4.9 shows that for the linear and square terms, the P-value is less than α, which means they have a more significant effect on the response. Two-way interaction term has little effect on IE.

Pareto chart (Fig. 4.19) demonstrates that only linear terms significantly impact the inhibition efficiency. Squared terms for temperature (X_1^2) and concentration (X_2^2) are having no noticeable impact on the inhibition efficiency, and the response does not influence the two-way interaction term (X_1X_2). Value of coefficient (R^2) acquired for the predicted model was 0.9894, which indicated the best fit expected model for experimental values[162]. Therefore, the output can be easily interpreted by the model.

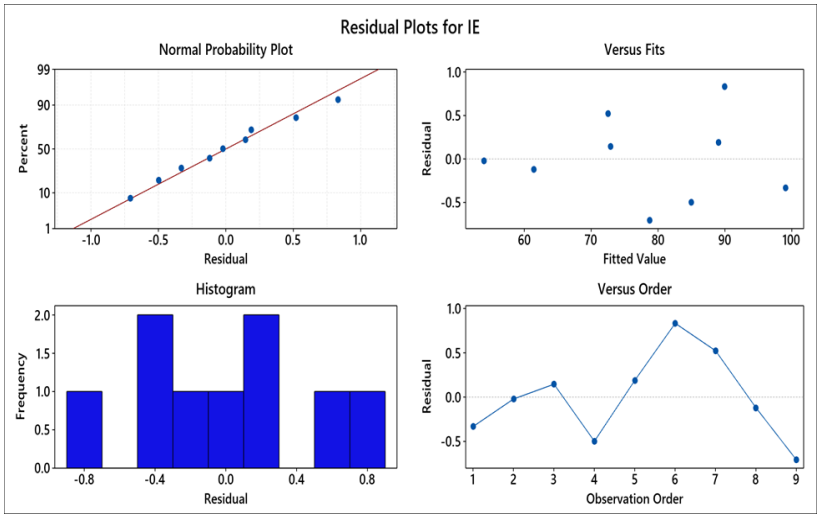

Fig. 4.18: Residual plots for inhibition efficiency

The impact of two parameters measured individually on IE% is plotted in the Main effects plots (Fig. 4.20). The figure shows that as CPE concentration increased from 1 to 5 v/v %, IE% also increased. It may be due to the coverage of active sites on the surface of mild steel metal with surplus CPE molecules. The type of adsorption exhibited by CPE molecules was physisorption because IE% decreased in higher temperatures. The results are precisely agreed with weight loss measurements.

Table 4.9: Analysis of variance for corrosion inhibition efficiency

Source	DF	Adj SS	Adj MS	F-Value	P-Value
Model	5	1667.74	333.549	527.87	0.000
Linear	2	445.32	222.660	352.38	0.000
Temp	1	256.15	256.150	405.38	0.000
Conc	1	189.17	189.169	299.37	0.000
Square	2	26.92	13.461	21.30	0.017
Temp*Temp	1	8.21	8.215	13.00	0.037
Conc*Conc	1	18.71	18.707	29.60	0.012
2-Way Interaction	1	5.86	5.856	9.27	0.056
Temp*Conc	1	5.86	5.856	9.27	0.056
Error	3	1.90	0.632		
Total	8	1669.64			

DF: degrees of freedom, Adj SS: adjusted sum of squares, Adj MS: adjusted mean of squares, F: Fischer's F-test value, P: probability

Interdependence of the parameters on the IE% was evaluated by plotting a contour and 3-D surface plot against two independent parameters in Fig. 4.21 a) and b),

respectively. It showed that the maximum corrosion inhibition efficiency was found for 5 v/v% concentration of CPE at 313 K. It can be attributed that elevated temperature causes an increase in the corrosion rate and obviously decreases the corrosion inhibition efficiency.

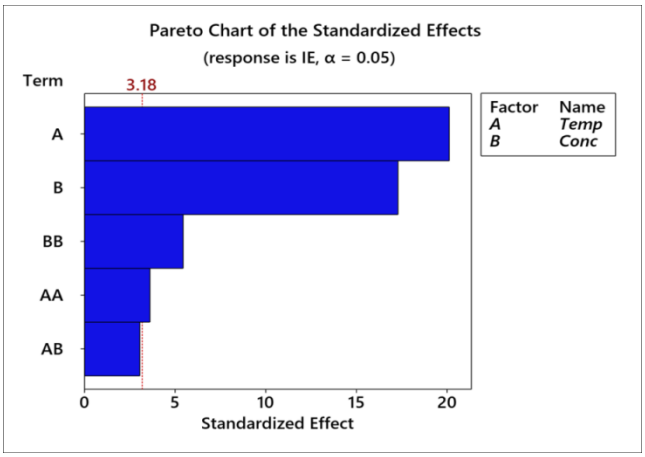

Fig. 4.19: Pareto chart of the standardized effects of mild steel

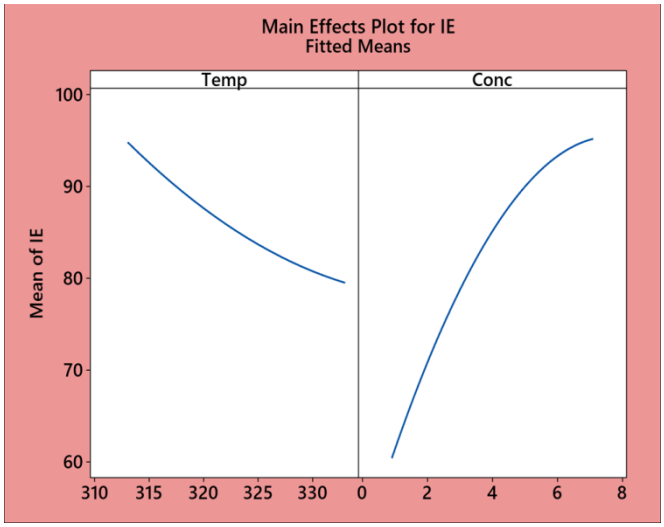

Fig. 4.20: Main effects plots for inhibition efficiency of mild steel in 0.5 M H_2SO_4

❖ ***Response Optimization***

Response optimization was performed to obtain the concentration of CPE and temperature at which a lower corrosion rate of mild steel in 0.5 M H_2SO_4. The maximum inhibition efficiency was investigated using the desirability function method by optimizing independent parameters presented in Fig. 4.22. The optimum temperature and

concentration parameters were 313 K and 5 v/v %, which yields the best result for the response of 99.06% inhibition efficiency.

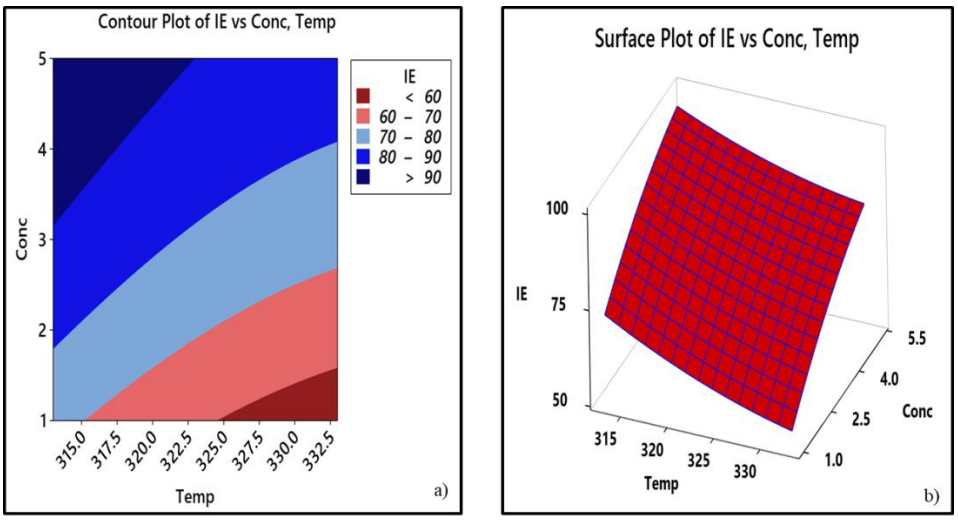

Fig. 4.21: a) Contour and b) 3-D surface plot for corrosion inhibition efficiency

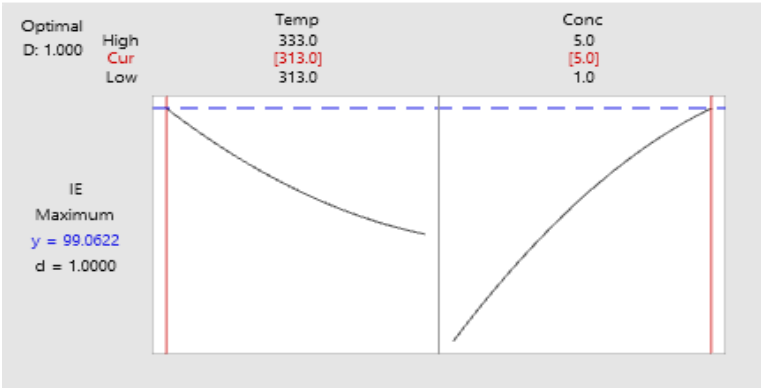

Fig. 4.22: Response optimization plot for inhibition efficiency

Conclusions

- Most of the tested metal salts exhibit good binding efficiency with CPE, which shows that they may be used to detect metal salts in different water sources.
- CPE behaves like an outstanding green corrosion inhibitor for mild steel in acidic environments.
- Weight loss studies reinforce the development of a protective barrier by CPE on the mild steel surface.

- Maximum inhibition potency of CPE in 1 M HCl and 0.5 M H_2SO_4 was calculated as 86.45% and 98.09%, respectively.
- The higher inhibition power in 0.5 M H_2SO_4 than 1 M HCl medium may attribute to the more adsorbed organic molecules of CPE on mild steel in 0.5 M H_2SO_4 medium than in 1 M HCl.
- Corrosion resistance power of CPE increases on adding the inhibitor concentration and decreases in elevated temperatures.
- The adsorption studies of CPE showed that it obeys Langmuir adsorption isotherm.
- CPE acts as a mixed-type inhibitor.
- Theoretical calculations of chief components of CPE such as neocrotocembraneic acid and stigmasterol are also establishing the corrosion inhibition potential of CPE.
- Predicted inhibition efficiency of CPE at various inhibitor concentrations and temperatures in 0.5 M H_2SO_4, investigated by RSM, was in agreement with the results obtained in weight loss measurements.